System-level modeling and simulation of the cell culture microfluidic biochip ProCell

Minhass, Wajid Hassan; Pop, Paul; Madsen, Jan; Hemmingsen, Mette; Dufva, Hans Martin

Published in:
2010 Symposium on Design Test Integration and Packaging of MEMS/MOEMS

Publication date:
2010

Document Version
Publisher's PDF, also known as Version of record

DTIP 5-7 May 2010, Seville, Spain

System-Level Modeling and Simulation of the Cell Culture Microfluidic Biochip ProCell

Wajid Hassan Minhass†, Paul Pop†, Jan Madsen†, Mette Hemmingsen‡, Martin Dufva‡
†Department of Informatics and Mathematical Modeling
‡Department of Micro- and Nanotechnology
Technical University of Denmark, DK-2800 Kgs. Lyngby
email: whmi@imm.dtu.dk

***Abstract*-Microfluidic biochips offer a promising alternative to a conventional biochemical laboratory. There are two technologies for the microfluidic biochips: droplet-based and flow-based. In this paper we are interested in flow-based microfluidic biochips, where the liquid flows continuously through pre-defined micro-channels using valves and pumps. We present an approach to the system-level modeling and simulation of a cell culture microfluidic biochip called ProCell, Programmable Cell Culture Chip. ProCell contains a cell culture chamber, which is envisioned to run 256 simultaneous experiments (viewed as a 16 x 16 matrix). We use an inverted fluorescence microscope to observe the experiments in real-time, allowing kinetic data analysis. We are able to automatically adjust the current experimental setup thus allowing, for the first time, *conditional experiments*. We propose a biochip architecture model and a comprehensive fault model that captures permanent faults occurring during chip operation. Using the proposed modeling and simulation framework, we perform an architectural level evaluation of two cell culture chamber implementations. A qualitative success metric is also proposed to evaluate chip performance in the presence of partial failures. Our results show that significant improvements in efficiency can be obtained using redundancy, providing improved chances to complete an experiment even in the presence of faults. This decreases the experiment repetition rate while increasing system productivity, saving time and reducing costs.**

I. INTRODUCTION

During the last decade, microfluidic biochips have become an actively researched area [1]. By miniaturizing the macroscopic chemical and biological processes to a sub-millimeter scale, microfluidic systems enable the integration of various assays onto a single chip. The technology is referred to as lab-on-a-chip (LoC), as it offers a promising alternative to a conventional biochemical laboratory. In addition to the reduced geometrical dimensions, this miniaturization also results in reduced required reagent volumes, saving material costs. Moreover, because of the homogeneous reaction conditions at the micro level, microfluidic-based systems provide results of enhanced precision compared to the conventional biochemical analyzers [2].

This work was supported by Grant No. 2106-08-0018 "ProCell", under the Programme Commission on Strategic Growth Technologies, the Danish Agency Agency for Science, Technology and Innovation.

There are two technologies for the microfluidic biochips: droplet-based [4] and flow-based [7]. Droplet-based biochips, also referred to as digital biochips, deal with discrete droplets on a two-dimensional electrode array and have so far been the focus of attention of the design automation community [5] [6]. In flow-based microfluidic biochips, the liquid flows continuously through pre-defined micro-channels using valves and pumps [7]. These flow-based biochips are fabricated using multilayer soft lithography techniques. Although the soft lithography technology has advanced faster than Moore's law [9], the design methodology of these biochips is still based on the bottom-up customized approach involving multiple manual steps with minimum design automation. Each new chip is designed by creating and connecting the on-chip components based on the precise steps of a specific assay [14], thus the chips are termed as "Full Custom" biochips.

As the designs become larger and more complex, the current bottom-up full-custom design approach will not scale to the new designs, widening the gap between the manufacturing technology capability and the achieved design complexity. New top-down computer-aided design tools are required, which can offer the same level of support as the one taken for granted currently in the semiconductor industry [10].

As a first step, we need to model the biochemical applications separately from the architecture. Thies et al. [12] propose a software system called *BioStream* with two levels of abstraction for describing biological assays. The first layer consists of a BioStream library, which is used to write a program for describing the assay. The second abstraction layer, a fluidic instruction set architecture (ISA), interfaces the first level with the underlying biochip architecture. Their work serves as a first step for decoupling the architecture from the assays.

Amin et al. [11] propose a general-purpose microfluidic architecture called AquaCore and an instruction set (consisting of instructions, such as, <*input id2, id1*>and <*mix id, time*> where *id1* is an input port, *id2* is a reservoir and *id* is the mixer) to be implemented on this architecture. AquaCore can be programmed to run any assay, and is thus termed as programmable LoC (PLoC). Although such a general-purpose PLoC has the obvious advantage of fast

 ISBN: 978-2-35500-011-9

turnaround time and lower cost (due to production in larger quantities compared to the full custom biochips), it has a key concern of reliability (valves operate reliably only for a few thousands of actuations), as reported in the paper. Furthermore, considering the vast variety in the biochemical applications in terms of the biochip architectural requirements, it is not possible to run all these applications on one architecture. Even if it is assumed that all these applications can be run by a generic PLoC, it is very difficult to achieve a reasonably high efficiency for all these applications from the same architecture.

Considering the above facts and the low cost of the manufacturing process (soft lithography) [8] for the flow-based microfluidic biochips, it is more suitable to develop application-specific architectures providing a compromise between full custom and general-purpose architectures. These application-specific programmable LoC (ASPLoC) can be tailored to provide a higher efficiency for a specific set of applications bringing it closer to the full custom biochips, while retaining the advantages of lower cost and flexibility of the general purpose PLoCs.

Modeling and simulation of the LoC systems are imperative for quickly evaluating design decisions without building costly prototypes. The simulations can be carried out at different levels of abstraction. Chakrabarty et al. [10] propose hierarchical modeling and simulation framework for the LoC systems, from the component-level to the system-level. The system level involves system performance modeling and behavioral simulation of the system operation. The system model needs to be complemented by component models in order to characterize the individual microfluidic component behavior, and to emphasize the physical properties and the relationships at the circuit level. Wang et al. [18] present a schematic-based approach to model and simulate the LoC systems using theoretical microfluidic models for the components. They use parameterized and closed-form models of the LoC elements to perform both DC and transient analysis of the chip. Using the analyses, they propose to capture the influence of topology, element sizes, and material properties on the biochip performance. Amin et al. [13] propose computer-aided design support methods for the microfluidic biochips at the physical design level. They propose methods to automatically infer the control valve placement, reducing the number of control lines needed to drive the valves and for routing these valves to the control ports.

In this paper, we present an approach for the high level modeling and simulation of a cell culture microfluidic biochip called ProCell, Programmable Cell Culture Chip [15]. ProCell is envisioned to run up to 256 experiments simultaneously. We use an inverted fluorescence microscope to observe the experiments in real-time. Depending on the observed outcome of a particular experiment, we are able to automatically adjust the current experimental setup. Thus, for the first time to our knowledge, *conditional experiments* can be performed.

ProCell can be viewed as an ASPLoC as it can be used to implement a specific set of applications with reasonably high efficiency, e.g., in vitro drug testing, genomics, stem cell analysis, tissue engineering [15]. This would offer the possibility of breakthroughs in regenerative medicine, cancer research and developmental biology.

Biochips belong to the class of Micro-Electro-Mechanical Systems (MEMS) and exhibit many different types of faults. Modeling these faults and their impact is imperative in order to perform a realistic system analysis.

In this paper we propose a biochip architecture model and a comprehensive fault model. We model faults that cause partial failures in the chip during operation and propose a success metric Q, which provides a qualitative measure of the chip performance in the presence of partial failures. Using the proposed simulation framework, we provide an architectural-level comparison of two cell culture chamber implementations. Our results show that significant improvements in efficiency can be obtained using redundancy, providing improved chances to complete an experiment even in the presence of faults. This decreases the experiment repetition rate while increasing system productivity, saving time (one cell culture experiment can take many days to complete), and reducing costs, since the purified proteins and compounds used in the experiments are highly expensive.

The rest of the paper is organized as follows. Section II describes the details of the ProCell prototype operation. Section III.A presents the architecture model of the cell culture biochip and Section III.B gives details of the proposed fault model. Different redundancy schemes are discussed in Section III.C and Section III.D gives out the problem formulation. The simulation framework is presented in Section IV. Section V describes the experimental results and Section VI presents the conclusions.

II. PROCELL PROTOTYPE OPERATION

ProCell is a new microfluidic-based device (being developed at the Technical University of Denmark, DTU) for culturing and monitoring of living cells in real-time [15]. ProCell is aimed to be a powerful, user-programmable, completely self-contained open platform for performing high throughput conditional cell culture experiments.

The ProCell chip contains one large chamber with 16 inlets and 16 outlets. There are a total of 32 individual inlets carrying soluble compounds (e.g., growth factors), which connect to the chamber inputs through 16 independent two-way valves. ProCell cell culture chamber is a modified version of the well characterized single experiment culture chamber developed at DTU [16]. Fig. 1 shows an example of a large chamber being divided into 8 virtual cell culture chambers using the laminar flow property of liquids at micro scales (each row can be viewed as a virtual chamber). Laminar flow is a distinguished category in the liquid flow classification [3]. Laminar flows are defined as the flow of fluids in parallel layers without any disruption between the layers. To carry out the experiment, first, valve D2 is opened and valve D1 is closed, allowing 8 different cell types to be pumped into the large chamber and since laminar flow conditions are applied eight corresponding stripes of cells are produced. After sedimentation, cells adhere to the bottom of the chip.

 ISBN: 978-2-35500-011-9

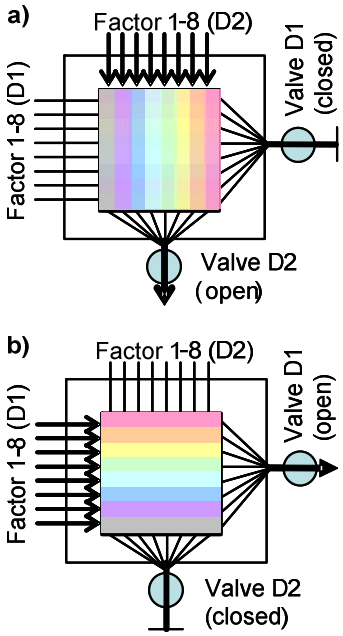

Figure 1: ProCell: Laminar flow-based large chamber

Then, valve D2 is closed and valve D1 is opened, allowing eight soluble compounds to perfuse over the cells in the perpendicular direction creating simultaneous experiments in the chip. Exposure of a cell colony to the soluble compound and monitoring its reaction is termed as an experiment. Since we have 8 cell colonies in each virtual chamber and there are 8 virtual chambers in total, thus we have 64 simultaneous experiments taking place in the chip. The fluid flow is managed by pumps that are controlled by electric motors.

A. *Large Chamber vs Isolated Chambers*

Fig. 1 shows a large chamber that is divided into 8 virtual chambers. Each chamber holds 8 cell colonies. Dividing the large chamber in such a way allows the in vitro conditions in the virtual chambers to resemble more closely to the natural in vivo conditions, since the cells are placed next to each other both horizontally as well as vertically.

A second choice of chamber architecture is to use 8 independent chambers physically isolated from each other. Just like the virtual chambers in the previous case, each isolated chamber also holds 8 cell colonies. The difference in this case is that the cells are placed next to each other only horizontally. Vertically, the isolated chambers have solid boundaries, i.e., each row (representing a chamber) is isolated from the rows next to it. Although such a scheme may have less resemblance with the natural conditions, it may prevent faults in one chamber, such as air bubbles, from advancing to the other chambers. We analyze the performance of both kinds of chamber implementations in this paper.

B. *Conditional Experiments*

The current ProCell prototype is able to run up to 64 experiments simultaneously. We use an inverted fluorescence microscope to observe the experiments in real-time, allowing kinetic data analysis. Depending on the observed intermediate outcome of a particular experiment through optical feedback, we are able to automatically adjust the current experimental setup thus creating *conditional experiments*.

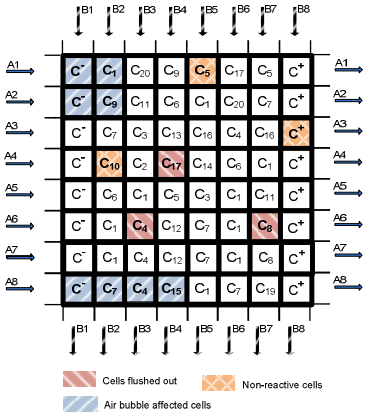

Figure 2: Biochip Architecture Model

ProCell uses the Zeiss AxioObserver Z1 inverted fluorescence microscope [19] for real time image capturing of the cell culture chamber over extended periods of time. The microscope is integrated with a Fujitsu high-end workstation CELSIUS R650. MCL-D2568 [20].

III. SYSTEM MODEL

A. *Biochip Architecture Model*

Fig. 2 shows the biochip architecture model. Each row in the model represents a chamber[1]. The architecture is represented by an 8x8 matrix (8 rows representing 8 chambers, where each chamber hosts 8 cell colonies). Each element of the 8x8 matrix hosts a cell colony, i.e., a separate experiment.

One primary step common to all cell culturing applications is the placement of cell colonies onto the chambers. In Fig. 2, 20 different cell colonies ($C_1 - C_{20}$) are placed on the biochip. The cell colonies marked with different patterns represent the fault affected regions, see next section. Each cell culture experiment requires some sort of controls to ensure quality of compounds being inserted into the chamber (which may degrade over time since one experiment lasts for many days) and to guarantee that the conditions in the chamber (e.g., a certain compound concentration) are uniform (some cell colonies might consume the compound at a rate fast enough to deprive the cell colonies downstream of it, creating undesired non-uniform conditions). Positive and negative controls, provided by specific cell colonies depending on the application, are used for this purpose [17]. Cell colonies serving as positive controls are manipulated to give out positive signals (e.g., certain level of fluorescence) in the presence of desired conditions (e.g., desired concentration of the compound) and are placed as the last cell colony in the chamber as shown in Fig. 2 using notation C^+. Absence of a positive signal from a positive control means

[1] In the rest of the paper, the chamber will be used interchangeably for the virtual or isolated chamber (not for the large chamber).

that the chamber no longer holds the desired conditions and the experimental results of that chamber are no longer reliable. Cell colonies serving as negative controls are manipulated to give out negative signals (e.g., absence of a certain level of fluorescence) in the presence of desired conditions (e.g., desired quality/ concentration of the compound) and are placed as the first cell colony in the chamber as shown in Fig. 2 using notation C^{-}. A negative control giving positive results also renders the chamber experimental results unreliable.

Different cell colonies can exhibit different properties in a chip and are thus placed at different locations in the chamber, based on the application. Some cell colonies (termed as *Comm* – communicator colonies) secrete compounds that are useful for the cell colonies placed downstream. Such colonies are placed close to the chamber inlets. It may also be possible that these secretions are instead harmful for the other cell colonies, in which case the cell colonies secreting these compounds are placed close to the outlets ensuring that they do not contaminate the chamber. Some cell colonies might be very rare or very expensive (and thus are considered high priority – *HP*) and would hence be placed at the location most suited to their requirements, making a compromise on the placement of other cell colonies (considered low priority – *LP*). *HP* and *LP* can also reflect the weight of a particular combination of cells and experimental conditions in a chamber, since some combinations may be more vital than others in order to test a certain hypothesis. The cell colony placement scheme (the order in which the colonies are placed) on a chamber is thus dependent on the properties of the cell colonies and the desired output of the experiments being run on the chip. Placement scheme can have an impact on the tolerance to faults, e.g., colonies placed close to the inlets are more susceptible to air bubbles than the ones placed close to the outlets.

Based on the cell colony properties, the colonies placed on the chip in Fig. 2 are categorized as:

- Negative Control (–): C^{-}
- Positive Control (+): C^{+}
- *Comm*: C_2, C_6, C_{12}, C_{17}
- High Priority (*HP*): $C_1, C_4, C_9, C_{10}, C_{15}$
- Low Priority (*LP*): All others

B. Fault Model

As discussed in Section II.B, there are 64 simultaneous experiments running on the chip, i.e., each cell colony represents a different experiment. Failure of an experiment caused by a fault is defined as a cell colony being unable to exhibit the reactive response, which it would exhibit otherwise under the applied conditions in the absence of that fault.

Different kind of faults can occur in a cell culture biochip. Some faults (e.g., mechanical pump breakdown, electronic motor failure) result in the failure of all the cell colonies in a chamber (complete chamber failure), whereas others (e.g., air bubbles enclosing one cell colony in the chamber thus modifying its conditions) may lead to the failure of some of the cell colonies in the chamber, i.e., a partial chamber failure. In this paper we model partial failures in the chip and propose a metric called Failure Index (FI) which is used to provide a qualitative success measure of the biochip performance in the presence of partial failures.

TABLE 1
FAULT TYPES

Cause	Fault	Error	Impact	Possible Failure Grade
Air bubbles	Cells in the chamber enclosed in air bubbles	Cells enclosed in air bubbles no longer affected by the compound inserted into the chamber	Complete or partial chamber failure	*FC* *C* *PH* *PL*
Over-stressed cells	None or partial cell adhesion	Some cells in some chambers flushed out with the media	Complete or partial chamber failure	*FC* *C* *PH* *PL*
Over-stressed cells	Cells no longer react in a normal manner	None or incorrect results which will not be reproduced upon repetition	Complete or partial chamber failure	*FC* *C* *PH* *PL*

A quantitative measure of success of the biochip can be the total number of experiments run on the biochip without failure. However, the cell colonies placed on the biochip have different properties and failure of one cell colony may have a stronger impact compared to the other, e.g., failure of the negative control would result in the failure of the whole chamber. Thus a qualitative measure of success is required.

Table 1 presents the three most common faults that occur in cell culture biochips together with the corresponding errors and possible failure grades. Failure grade assignment is done to all 64 cell colonies on the biochip depending on the kind and/or number of cell colonies affected by the fault. Failure grade *PL* or *PH* is assigned if the fault occurs on a low priority or a high priority cell colony, respectively. If the fault occurs on a communicator colony or on all the negative/ positive controls available in a chamber, failure grade *PH* is assigned to all the colonies in the chamber marking a complete chamber failure. Failure grade *CC* is a chamber level failure grade marking complete chamber failure and *FC* is a chip level failure grade representing full chip failure.

Table 2 shows the value contributed by the fault type to the total Failure Index metric depending on the failure grade assigned to the fault. For example, a single *PL* grade failure contributes 1 failure point, whereas a high priority cell colony failure resulting in a *PH* grading contributes 2 failure points. Failure of the positive or negative controls or a communicator colony is ranked as a complete chamber failure equivalent to 16 failure points. Last column of Table 2 shows the range of *PL* failure index contribution for a chamber as {0-5, 16}. This represents that that if 5 cell colonies out of the 6 in a chamber (2 cell colonies are reserved for positive and negative controls) undergo partial failure, the failure index contribution is 5 points, whereas partial failure of all 6 colonies is ranked as a complete chamber failure equivalent to 16 failure points. Same ap-

 ISBN: 978-2-35500-011-9

plies for the failure index contribution of *PH* failure shown in the Table. Using different failure index contributions for different impacts allows qualitative evaluation of chip failure.

TABLE 2
FAILURE INDEX

Fault Impact	Failure Grade	Description	Failure Index Contribution
Partial Chamber Failure	*PL*	Represents partial chamber failure, *L* in *PL* represents failure of low priority cells	1 / Each low priority cell experiment failure in the chamber [0 – (*M*-*l*-1)[1], 2*M*]
	PH	Represents partial chamber failure, *H* in *PH* represents failure of high priority cells	2 / Each high priority cell experiment failure in the chamber (0 – 2×(*M*-*l*-1), 2*M*)
Complete Chamber Failure	*CC*	Represents complete failure of a chamber (e.g., loss of positive/negative control or the *Comm*)	2*M*
Full Chip Failure	*FC*	Represents simultaneous complete failure of all chambers	$N^1 \times 2M$

The Failure Index of a chip is calculated by adding the failure index contributions (*FIC*) of all chambers:

$$FI = \sum_{i=1}^{N} FIC_i \quad (1)$$

where *N* is the number of chambers.

In order to calculate *FIC* of a chamber, first the failure grade of the fault is determined based on the cell colony type at which the fault occurs. Based on the failure grade, the *FIC* for chamber 1 can be calculated as,

$$FIC_1 = \left\lceil \sum_{i=1}^{M} PH_i \right\rceil + \left\lceil \sum_{i=1}^{M} PL_i \right\rceil \quad (2)$$

where *M* is the number of cell colonies in the chamber, *PH* represents the failure points contributed by any high priority cell failures in the chamber, and *PL* represents the failure points contributed by the low priority cell failures. The roof value for the first term is 2*M* (16 in this case) which is applied in case the summation value exceeds (*M*–*l*–1), where *l* is the number of cell colonies reserved for the positive and negative controls in the chamber. The roof value for the second term is also 2*M* and is applied if the summation value exceeds 2×(*M*–*l*–1).

In Fig. 2, chamber 1 (marked with inlet A1) has an air bubble failure on C^-. Loss of the negative control marks a complete chamber failure, thus FIC_1 = 16. In chamber 6, cell colonies C_4 and C_8 fail to adhere to the chip and are flushed out. C_4 and C_8 are in categories *HP* and *LP* respectively. As per eq. 2, FIC_6 is calculated as (2 + 1) = 3. Similarly, FIC_2, FIC_3, FIC_4, and FIC_8 are equal to 16. FIC_5 and FIC_7 are equal to 0. Failure Index of the whole chip is equal to sum of all *FIC* (1), i.e., 83 for this case. In the worst-case, *FI* is represented by a full chip failure (*FC* in Table 2).

The success metric Q is thus calculated as,

$$Q = \left[\frac{N \times 2M - FI}{N \times 2M}\right] \times 100 \quad (3)$$

where *N* and *M* represent the number of chambers and the number of cell colonies in a chamber, respectively. For the current case, Q is (128 – 83) / 128 = 35.15%.

Note that chamber 6 and chamber 7 in Fig. 2 have the same placement scheme. Chamber 6 is affected with partial failures, whereas chamber 7 is fault free. The redundancy increases the success probability for that particular placement scheme. The redundancy schemes are discussed in the next section.

The faults listed here are permanent faults that occur during chip operation and are detected through optical feedback in real time. Based on the detection results, the experimental setup is adjusted to cater for the caused errors. Fault detection is not a part of the ProCell simulator since the faults are randomly generated and injected into the cell culture chamber during simulation. The simulator is used to architecturally compare two different cell culture chamber implementations.

C. Redundancy Schemes

Different redundancy schemes can be introduced into the chambers in order to improve the chip reliability. Two types of redundancy schemes are proposed here: *placement redundancy* and c*ontrol redundancy*.

Placement redundancy is defined as placement of the same cell colonies in multiple chambers, i.e., the colony placement done in one chamber is repeated in multiple chambers. The number of chambers in which the same placement is repeated is termed as the redundancy level.

In this paper, two types of chamber implementations are under consideration as discussed in Section II.A. The primary difference between the two implementations, in terms of fault impact, is that in the virtual chambers (present in one large chamber) the air bubbles can easily spread from one chamber to the other.

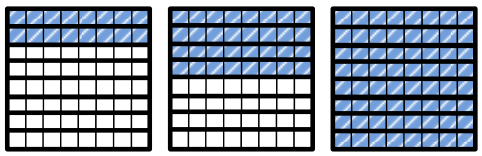

Figure 3: Placement Redundancy: 8 Isolated Chambers

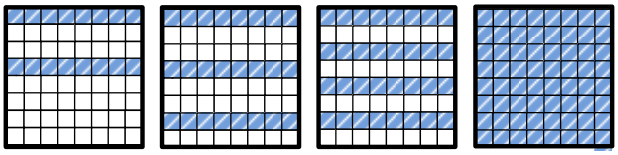

Figure 4: Placement Redundancy: Large Chamber (8 Virtual Chambers)

[1] *N* is the maximum number of chambers and *M* is the maximum number of cell colonies per chamber. In this case, *N* = *M* = 8. *l* is the number of colonies used for positive and negative controls per chamber, in Fig. 3 *l* = 2.

However, this is not true for the isolated chambers since those are separated from each other using solid boundaries. Fig. 3 shows the placement redundancy schemes for the isolated chambers implementation. Fig. 4 shows the placement redundancy schemes for the virtual chambers. Maximum air bubble radius is set to three chambers. For redundancy levels 1 and 2 in Fig. 4, the redundant placements are made 2 chambers apart such that the air bubble affecting one chamber does not affect the other redundant chambers even in the worst-case.

Control redundancy is defined as placing multiple control colonies on a single chamber, e.g., instead of one negative control two negative controls can be placed on the chamber. Failure of the control marks the failure of the whole chamber. Thus, the placement of redundant controls can increase the success probability of the experiment.

D. Problem Formulation

The problem addressed can be formulated as follows. Given (1) a cell culture biochip architecture model $\mathcal{M}$ consisting of an $N \times M$ matrix representing the cell culture chamber, (2) a set of three different static cell colony placement schemes $\mathcal{P}$, (3) a fault model $\mathcal{F}$ together with the set of occurrence rates of different faults, and (4) a set of placement redundancy levels $\mathcal{R}$, the target is to perform an architectural level evaluation of two implementations: large chamber (with virtual chambers) vs isolated chambers. The evaluation provides qualitative measure of success Q for each chamber implementation under the same conditions. The evaluation is made at different redundancy levels in both cell culture chamber implementations in order to determine the variation in Q.

The architectural evaluation involves mapping the placements $\mathcal{P}$ onto the chamber architecture model, conducting a property analysis of the placed cell colonies, randomly generating different faults according to the given occurrence rates (see Section V for details) and calculating the failure index FI which is used to calculate Q. The performance evaluation is based on the properties of the architecture model, the fault model and the cell colonies at which these faults occur. The architectural comparison is performed independent of any specific application rendering the results equally applicable to all applications that can be executed on the chip.

IV. PROCELL SIMULATOR

The simulation framework is shown in Fig. 5. Cell chamber implementation choice, the placement scheme, fault rates and selected redundancy levels are given as an input to the simulator.

The first step in the simulator operation is to map the selected placement onto the selected chamber implementation. The chamber implementation is represented as a matrix model in the simulator. Different cell colonies have different properties and thus different priority levels as discussed in Section III.A. Based on the properties of these cell colonies, a new property matrix is generated next. This property matrix is utilized at the time of failure index evaluation since the same fault occurring on cell colonies with different properties can result in a different failure index contribution.

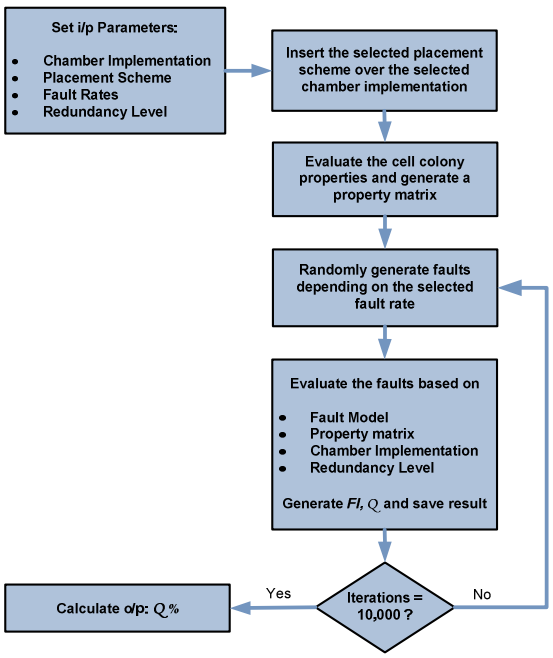

Figure 5: Simulation Framework

Next, using Monte Carlo Simulation (MCS), faults are randomly generated based on the chosen fault rates and evaluated to generate the Failure Index (*FI*) and the success metric Q. *FI* calculation takes into account the fault model built in the simulator, the generated property matrix, selected chamber implementation and the chosen redundancy level. At the end of the MCS cycle (10,000 runs), the average percentage value of Q is calculated and generated as an output.

Next, using Monte Carlo Simulation (MCS), faults are randomly generated based on the chosen fault rates and evaluated to generate the Failure Index (*FI*) and the success metric Q. *FI* calculation takes into account the fault model built in the simulator, the generated property matrix, selected chamber implementation and the chosen redundancy level. At the end of the MCS cycle (10,000 runs), the average percentage value of Q is calculated and generated as an output.

V. EXPERIMENTAL RESULTS

Table 3 shows the results of the architectural comparison (as a measure of Q) between the two chamber implementations using varying fault rates. Only control redundancy is utilized for this comparison. The property based description of the three placement schemes is as follows:

$P1 = <\!-, Comm, LP, \quad LP, LP, LP, \ LP, +\!>$
$P2 = <\!-, Comm, LP, Comm, LP, LP, \ HP, +\!>$
$P3 = <\!-, \quad - \quad , LP, Comm, LP, LP, HP, +\!>$

TABLE 3
RESULTS: PERFORMANCE COMPARISON

Fault Rate	*P*1	*P*2	*P*3
8 Isolated chambers			
(10,5,5)	55.14	54.19	58.53
(20,5,5)	38.08	36.72	41.26
8 virtual chambers (Max air bubble radius = 3 chambers)			
(10,5,5)	44.25	43.15	48.02
(20,5,5)	23.30	21.58	25.66
8 virtual chambers (Max Air bubble radius = 5 chambers)			
(10,5,5)	36.36	34.96	39.96
(20,5,5)	15.27	13.93	17.52

TABLE 4
8 ISOLATED CHAMBERS: REDUNDANCY RESULTS

Fault Rate	Redundancy	*P*1	*P*2	*P*3
(10,5,5)	2	79.60	71.40	81.09
(20,10,10)	2	46.30	32.80	47.11
(30,15,15)	2	22.97	12.47	23.61
(40,20,20)	2	10.33	4.25	10.50
(10,5,5)	4	95.14	91.37	95.86
(20,10,10)	4	69.86	54.16	71.24
(30,15,15)	4	40.07	23.41	41.37
(40,20,20)	4	18.93	7.89	19.31
(50,25,25)	4	7.75	2.25	7.92
(10,5,5)	8	99.27	98.80	99.60
(20,10,10)	8	88.38	78.15	90.01
(30,15,15)	8	62.53	40.96	64.06
(40,20,20)	8	33.47	15.25	34.75
(50,25,25)	8	14.66	4.50	15.19

TABLE 5
8 VIRTUAL CHAMBERS: REDUNDANCY RESULTS

Fault Rate	Redundancy	*P*1	*P*2	*P*3
Maximum air bubble radius is 3 chambers for all cases				
(10,5,5)	2	74.46	64.55	75.90
(20,10,10)	2	37.53	24.69	38.26
(30,15,15)	2	16.49	8.13	16.92
(40,20,20)	2	6.45	2.4	6.67
(10,5,5)	3	83.19	74.20	84.87
(20,10,10)	3	43.54	28.33	44.44
(30,15,15)	3	18.45	8.83	19.10
(40,20,20)	3	7.00	2.46	7.20
(10,5,5)	4	87.41	79.75	89.27
(20,10,10)	4	49.08	32.33	50.57
(30,15,15)	4	21.06	9.89	21.59
(40,20,20)	4	7.70	2.61	13.64
(10,5,5)	8	95.82	92.41	96.71
(20,10,10)	8	66.87	49.16	69.58
(30,15,15)	8	33.33	16.71	35.02
(40,20,20)	8	12.85	4.36	13.67
(50,25,25)	8	4.23	0.97	4.50

As can be seen, *P*2 and *P*3 are identical, other than the fact that the *Comm* of *P*2 is replaced by an extra negative control in *P*3, providing the control redundancy.

Different fault rates can be chosen for the three types of faults discussed in Table 1. Fault rates under which the simulation experiments were performed are given in the first column in Table 3. Since no statistics on the fault occurrence rates are available yet, we base our experiments on the limited observations made during the ProCell operation. The experiments are carried out at different fault rates per experiment and the results are analyzed. Whenever more accurate statistics become available, those can easily be plugged into the simulator to perform architectural evaluation. The notation (10, 5, 5) in the first column of the Table means that the air bubble occurrence rate is 10%, rate of the faults resulting in cells not adhering to the chamber is 5% and the rate at which the cells become non-reactive is 5%, respectively.

Since the air bubbles are inserted into the chamber through inlets, the cell colonies closer to the inlets are more susceptible to the air bubble faults than the ones close to the outlets. We assume a linear decrease of 1% in the occurrence rate when moving from the inlets to the outlets in the chamber, i.e., cell colony closest to the inlet has a rate of 10%, next one has a rate of 9%, and so on.

As shown in Table 3, the isolated chambers have a higher success rate Q compared to the virtual chambers. As the fault rates increase, the gap in the success metric also widens. This is because in the virtual chambers the air bubbles can easily spread from one chamber to the other. However, this is not true for the isolated chambers since those are separated from each other using solid boundaries. Comparing results of *P*2 and *P*3, it can be seen that the control redundancy provides up to 5% increase in Q. Tables 4 and 5 show the variations in Q as a result of placement redundancies for the same placement schemes.

As shown in Table 4, even a level-2 placement redundancy provides up to 24% increase in Q (*P*1 under (10, 5, 5)) compared to the results without placement redundancy in Table 3 for isolated chambers. Q is calculated by using the average Q calculated over an MCS cycle (10,000 runs). For every run, the higher value of Q from the two redundant chambers (for level-2) is considered for calculating the average Q. The redundancy level can be increased to cater for the increasing fault rates. However, for the isolated chambers as shown in Table 4, the Q value falls below 35% when the fault rates go up to (40, 20, 20), even with a placement redundancy level of 8. For the virtual chambers, the results are shown in Table 5. At the placement redundancy level 8, Q goes as low as 35% at the fault rates (30, 15, 15).

The results show that the mixed redundancy scheme (both placement and control) provides the best results.

VI. CONCLUSION

In this paper we have presented a modeling and simulation framework for the cell culture microfluidic biochip ProCell. We have proposed a biochip architecture model and a comprehensive fault model capturing permanent faults that occur during the chip operation. Using the proposed simulation framework, we have carried out an architectural level evaluation of two cell culture chamber implementations. The proposed approach considers the fault model, cell placement scheme, fault occurrence rates, and the redundancy level and provides a qualitative success metric as a measure of performance for both architectures in the presence of partial failures. Three different cell place-

 ISBN: 978-2-35500-011-9

ment schemes have been used to evaluate the architectural performance under different redundancy levels and varying fault rates. Our results show that significant improvements in efficiency can be obtained by using redundancy schemes; increasing the system productivity, saving time and reducing costs. However, evaluation depicts that both architectures have separate limits of maximum tolerable fault rates, after which the redundancy is no longer effective in improving the chip performance.

REFERENCES

[1] E. Verpoorte and N. F. De Rooij, "Microfluidics meets MEMS", *Proceedings of the IEEE*, vol. 91, pp. 930-953, 2003.

[2] "*Bio-chips and chips for bio*", Report commissioned by MEDEA and Scientific Community, 2004. http://www.catrene.org/web/about/Biochips_ExecSumm_(2004).pdf Last accessed: 16th March, 2010.

[3] V. Ts. Vanchikov, "Special form of laminar liquid flow in hydraulic devices". *Russian Engineering Research*, vol. 28, no. 9, pp. 854–855. 2008.

[4] E. S. K. Cho, H. Moon, and C.J. Kim, "Creating, transporting, cutting, and merging liquid droplets by electrowetting-based actuation for digital microfluidic circuits," *Journal of Microelectromechanical Systems,* vol. 12, no. 1, 2003.

[5] K. Chakrabarty and J. Zheng, *Design automation methods and tools for microfluidic-based biochips*, Springer, 2006.

[6] E. Maftei, P. Pop, and J. Madsen, "Tabu search-based synthesis of dynamically reconfigurable digital microfluidic biochips", *Proceedings of the international conference on Compilers, architecture, and synthesis for embedded systems*, pp. 195-204, 2009.

[7] T. Thorsen, S. Maerki, and S. Quake, "Microfluidic largescale integration", *Sci*, 298:580-584, 2002.

[8] P.F. Xiao, N.Y. He, Q.G. He, Z.C. Liu, Z.H. Lu, "Soft lithography for oligonucleotide array fabrication", *Proceedings of the IEEE/EMBS*, 2001.

[9] J. Hong and S. Quake, "Integrated nanoliter systems," *Nature BioTechnology*, vol. 21, no. 10, pp. 1179–1183, 2003.

[10] T. Zhang, K. Chakrabarty and R. B. Fair, *Microelectrofluidic Systems: Modeling and Simulation*, CRC Press, Boca Raton, FL, 2002.

[11] A.M. Amin, M. Thottethodi, T.N. Vijaukumar, S. Wereley, and S.C. Jakobson, "AquaCore: a programmable architecture for microfluidics", *Proceedings of International Symposium on Computer Architecture*, pp. 254-265, 2007.

[12] W. Thies, J.P. Urbanski, T. Thorsen, and S. Amarasinghe, "Abstraction layers for scalable microfluidic biocomputing", *Natural Computing*, vol.7-2, pp. 255-275, 2008.

[13] N. Amin, W. Thies, S. Amarasinghe, "Computer-aided design for microfluidic chips based on multilayer soft lithography", *Proceedings of the IEEE International Conference on Computer Design ICCD*, 2009.

[14] A. ul Haque et al., "A MEMS fabricated cell electrophysiology biochip for in silico calcium measurements", *Sensors & Actuators: B. Chemical*, pp. 391–399. 2006.

[15] M. Dufva, H. Bruus, P. Pop, and J. Madsen, "ProCell – Programmable cell chip: Culturing and manipulation of living cells with real-time reaction monitoring", Technical Report, Technical University of Denmark, 2009.

[16] S. Petronis, M. Stangegaard, C. Christensen, and M. Dufva, "Transparent polymeric cell culture chip with integrated temperature control and uniform media perfusion". *Biotechniques*, 40, 368-376. 2006.

[17] A. Stacey and G. Stacey, *Routine quality control testing of cell cultures – Antiviral Methods and Protocols (Part 3),* Springer 2000.

[18] Y. Wang, R. Magargle, Q. Lin, J.F. Hoburg, and T. Mukherjee, "System-oriented modeling and simulation of biofluidic lab-on-a-chip", *Proceedings of the 13th International Conference on Solid-State Sensors and Actuators,* Vol. 2, pp. 1280–1283, 2005.

[19] "Zeiss AxioObserver Z1 for live-cell fluorescence imaging", Biological Imaging Facility, College of Natural Resources, University of California, Berkeley. http://microscopy.berkeley.edu/instruments/Z1.html Last accessed: 26th October, 2009.

[20] "Data sheet – Celsius R650. Your high-end workstation without compromise" Issue July 2009. https://sp.ts.fujitsu.com/dmsp/docs/ds_celsius_r650.pdf Last accessed: 26th October 2009.

 ISBN: 978-2-35500-011-9